An analytic redshift-independent formulation of baryonic effects on the matter power spectrum

Schaller, M.; Schaye, J.

Monthly Notices of the ROYAL ASTRONOMICAL SOCIETY

MNRAS **540,** 2322–2330 (2025) https://doi.org/10.1093/mnras/staf871
Advance Access publication 2025 May 28

An analytic redshift-independent formulation of baryonic effects on the matter power spectrum

Matthieu Schaller [1,2]★ and Joop Schaye [2]

[1]*Lorentz Institute for Theoretical Physics, Leiden University, PO Box 9506, NL-2300 RA Leiden, the Netherlands*
[2]*Leiden Observatory, Leiden University, PO Box 9513, NL-2300 RA Leiden, the Netherlands*

Accepted 2025 May 27. Received 2025 May 27; in original form 2025 April 16

ABSTRACT

Baryonic effects created by feedback processes associated with galaxy formation are an important, poorly constrained systematic effect for models of large-scale structure as probed by weak gravitational lensing. Upcoming surveys require fast methods to predict and marginalize over the potential impact of baryons on the total matter power spectrum. Here we use the FLAMINGO cosmological hydrodynamical simulations to test a recent proposal to approximate the matter power spectrum as the sum of the linear matter power spectrum and a constant multiple, $A_{\rm mod}$, of the difference between the linear and non-linear gravity-only power spectra. We show that replacing this constant multiple with a one-parameter family of sigmoid functions of the wavenumber k allows to us match the predictions of simulations with different feedback strengths for $z \leq 1$, $k < 3\,h\,{\rm Mpc}^{-1}$, and the different cosmological models in the FLAMINGO suite. The baryonic response predicted by FLAMINGO models that use jet-like active galactic nucleus (AGN) feedback instead of the fiducial thermally driven AGN feedback can also be reproduced, but at the cost of increasing the number of parameters in the sigmoid function from one to three. The assumption that $A_{\rm mod}$ depends only on k breaks down for decaying dark matter models, highlighting the need for more advanced baryon response models when studying cosmological models that deviate strongly from Lambda cold dark matter.

Key words: methods: numerical – cosmology: theory – large-scale structure of Universe.

1 INTRODUCTION

In the modern era of cosmology surveys, many probes [e.g. galaxy clustering, cosmic shear, cosmic microwave background (CMB) lensing, etc.] focus on detailed measurements of the distribution of matter in the Universe at multiple epochs and across different length scales. With the so-called Stage IV probes now starting to collect data, the onus is on the theorists to make accurate predictions that match the expected quality of the data. One of the particularly challenging aspects is the exploitation of information deep in the non-linear regime where perturbation theory is not sufficient anymore.

In addition to the non-linear gravitational evolution of the large-scale structure, predicting the effect galaxy formation processes and the feedback they induce on the matter density field is especially challenging. The modelling of these effects can be done via full hydrodynamical simulations of galaxy formation (e.g. Le Brun et al. 2014; McCarthy et al. 2017; Delgado et al. 2023; Pakmor et al. 2023; Schaye et al. 2023; Bigwood et al. 2025) but the immense computing resources that they require prevent their direct use in survey analysis pipelines. The community has thus turned towards semi-analytic models, often based on halo models (e.g. Semboloni, Hoekstra & Schaye 2013; Mead et al. 2015; Debackere, Schaye & Hoekstra 2020; Mead et al. 2020), or so-called baryonification models (e.g. Schneider & Teyssier 2015; Aricò et al. 2021; Ferreira et al. 2024). As such models can still be too slow to be used in cosmology parameter searches, they are often used to train emulators which are themselves fast enough (e.g. Aricò et al. 2021; Giri & Schneider 2021). With larger suites of hydrodynamical simulations starting to emerge, training such emulators directly on the output of simulations (e.g. Schaller et al. 2025) is a tempting prospect for forthcoming survey analysis. While these techniques can provide very accurate matches to simulations (typically 1 per cent accuracy up to $k \approx 10\,h\,{\rm Mpc}^{-1}$), it can be desirable to have simpler, analytic, approximations for the baryon effects on the matter power spectrum. Quick evaluation of the baryon response would extend its applicability to more areas, such as the construction of covariance matrices.

As part of their analysis, Amon & Efstathiou (2022) decomposed the total matter power spectrum as follows:

$$P_{\rm m}(k,z) = P_{\rm m}^{\rm L}(k,z) + A_{\rm mod}(k,z)\left[P_{\rm m}^{\rm NL}(k,z) - P_{\rm m}^{\rm L}(k,z)\right], \quad (1)$$

with the function $A_{\rm mod}(k,z)$ capturing the effect baryons have on the total matter power spectrum and $P_{\rm m}^{\rm L}(k,z)$, $P_{\rm m}^{\rm NL}(k,z)$ corresponding to the linear and non-linear matter power spectra. The case $A_{\rm mod}(k,z) = 1$ would lead to a model where the baryons have no effect on the matter density field.

Amon & Efstathiou (2022) then made two key assumptions about the function $A_{\rm mod}(k,z)$ they had just introduced:

(i) $A_{\rm mod}(k,z)$ does *not* depend on redshift.
(ii) $A_{\rm mod}(k,z)$ does *not* depend on the background cosmology.

★ E-mail: mschaller@lorentz.leidenuniv.nl

With these two assumptions, the total, baryon-corrected, matter power spectrum can thus be very easily evaluated as it only depends on the linear and non-linear (i.e. gravity-only) matter power spectra for which many rapid estimation techniques exist.

In their study, Amon & Efstathiou (2022) used a constant for the function $A_{\rm mod}(k, z)$ whose value was obtained by combining lensing and CMB data and requesting a consistent cosmology fit. In their follow-up study, Preston, Amon, & Efstathiou (2023) used a binned version of $A_{\rm mod}(k, z)$, where the value of $A_{\rm mod}$ in five different k-bins was obtained using a similar technique for different data set combinations. We extend this here by using an analytic function for $A_{\rm mod}$ rather than discrete bins.

The first of the remaining ingredients in equation (1), the linear matter power spectrum, $P_{\rm m}^{\rm L}(k, z)$, is traditionally obtained using Boltzmann solvers (e.g. Lewis, Challinor & Lasenby 2000; Lesgourgues 2011). The second ingredient, the non-linear power spectrum in a dark-matter-only (DMO) universe, $P_{\rm m}^{\rm NL}(k, z)$, is often expressed in terms of the non-linear boost to the linear power spectrum

$$\beta^{\rm NL}(k, z) \equiv \frac{P_{\rm m}^{\rm NL}(k, z)}{P_{\rm m}^{\rm L}(k, z)}. \tag{2}$$

Over the last two decades, various approaches have been proposed to compute this boost. The 'halo model' formalism (Seljak 2000; Smith et al. 2003; Asgari, Mead & Heymans 2023) proposes an analytic formalism with free parameters usually calibrated to the results of N-body simulations (e.g. Takahashi et al. 2012; Mead et al. 2016). More recently, interpolation between a large suite of DMO runs using various emulation techniques has started to compete with this approach (e.g. Heitmann et al. 2016; Lawrence et al. 2017; DeRose et al. 2019; Euclid Collaboration 2019; Bocquet et al. 2020; Angulo et al. 2021; Storey-Fisher et al. 2024; Chen et al. 2025).

With these two ingredients, the response of the matter power spectrum due to baryons can be expressed as

$$R(k, z) \equiv \frac{P_{\rm m}(k,z)}{P_{\rm m}^{\rm NL}(k,z)} \tag{3}$$

$$= \beta^{\rm NL}(k, z)^{-1} + A_{\rm mod}(k)\left[1 - \beta^{\rm NL}(k, z)^{-1}\right]. \tag{4}$$

Under the two assumptions listed above, $\beta^{\rm NL}(k, z)$ captures all the cosmology and redshift dependence, and $A_{\rm mod}(k)$ encodes the specifics of the galaxy formation model.

In this paper, we use the FLAMINGO suite of simulations (Kugel et al. 2023; Schaye et al. 2023) to obtain an analytic functional form for $A_{\rm mod}(k)$ that reproduces the data extracted from the runs using different strengths of stellar and thermal active galactic nucleus (AGN) feedback using a single free parameter. Expanding the study to models with jet-like AGN feedback, we find that the same function fits the results well at the cost of two extra free parameters. We then use our fits to verify whether the two key assumptions listed above hold for our simulations. In this process, we also identify the range of redshifts where the approximation holds, allowing the controlled use of our analytic fit within the analysis pipeline of modern surveys.

The FLAMINGO simulations have been shown to reproduce a series of observables of the galaxy and cluster population (McCarthy et al. 2023, 2025; Schaye et al. 2023; Braspenning et al. 2024, 2025; Kumar et al. 2025). As such, they are a great test bed to measure the effect of baryons on the matter power spectrum. Furthermore, the use of variations of the base model, where the observables have been systematically shifted in proportion to the estimated errors on the galaxy stellar mass function and cluster gas fractions (Kugel et al. 2023), allows for a direct connection between the baryonic response – here in the form of $A_{\rm mod}(k)$ – and the observables the simulations were calibrated to. Additionally, the simulations themselves have already been used to investigate the role of baryons on the so-called S8 tension (McCarthy et al. 2023, 2025; Elbers et al. 2025; Schaller et al. 2025).

This paper is organized as follows. In Section 2, we present the simulations used in this study. We then introduce our approximation in Sections 3.1–3.3 before testing the key assumptions in Sections 3.4 and 3.5. We generalize the model in Section 3.6 and summarize our findings in Section 4.

2 THE FLAMINGO SIMULATIONS

In this section, we provide a brief summary of the key components of the FLAMINGO simulations used in this study. The simulations and the strategy used to calibrate their free parameters are described in Schaye et al. (2023) and Kugel et al. (2023), respectively.

The simulations were performed using the open-source SWIFT simulation code (Schaller et al. 2024) In particular, neutrinos are evolved using the δf-method of Elbers et al. (2021) and the gas is evolved using the SPHENIX (Borrow et al. 2022) flavour of smoothed particle hydrodynamics.

The simulations include subgrid prescriptions for radiative cooling following Ploeckinger & Schaye (2020), an entropy floor at high densities and star formation using the method of Schaye & Dalla Vecchia (2008), the chemical enrichment model of Wiersma et al. (2009), and feedback from core collapse supernova using kinetic winds of Chaikin et al. (2023). Supermassive black holes are modelled using ingredients from Springel, Di Matteo, & Hernquist (2005), Booth & Schaye (2009), and Bahé et al. (2022). AGN feedback is modelled either as thermally driven winds (Booth & Schaye 2009) or by the collimated jet model of Huško et al. (2022).

The subgrid models were calibrated using a Gaussian process emulator, trained on a Latin hypercube of simulations, to predict the observables as a function of the free parameters of the subgrid models. A Markov Chain Monte Carlo (MCMC) search was then used in combination with the emulator to find parameters reproducing the $z = 0$ galaxy stellar mass function as well as the gas fractions in low-redshift groups and clusters inferred from X-ray and weak-lensing data, as detailed by Kugel et al. (2023). Besides generating sets of simulations parameters matching the data, they also constructed simulations where the target data are shifted by particular amounts with respect to observations. In particular, for the cluster gas fractions, they created different models where the observed gas fractions are shifted up and down compared to the results by $\pm N\sigma$, where σ is the scatter in the data (see Kugel et al. 2023, for the exact definitions). This procedure was performed for both AGN models.

All the simulations used in this study were run in a volume of 1 Gpc on the side, which is sufficient to obtain a converged baryon response of the matter power spectrum (Schaller et al. 2025). Apart from the runs used in Section 3.5, the simulations adopt as values of the cosmological parameters the maximum likelihood values from the DES year 3 data release (Abbott et al. 2022) combined with external probes, i.e. their '3×2pt + All Ext' model.[1]

The initial conditions were generated using the MONOFONIC code (Hahn, Rampf & Uhlemann 2021; Elbers et al. 2022) using a three-fluid formalism with a separate transfer function for each of the species.

[1]The parameter values are given in the first row of Table 2.

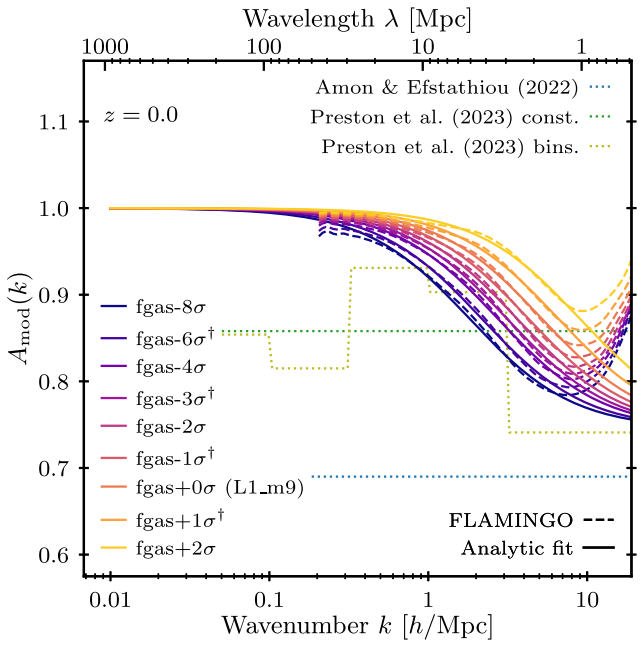

Figure 1. The function $A_{\rm mod}(k)$ at $z = 0$ extracted from the FLAMINGO simulations without jet AGN calibrated to different observed gas fractions (dashed lines), or the emulator of Schaller et al. (2025) (indicated by a dagger) for intermediate gas fractions where no simulation was run. The solid lines in matching colours show the analytic fitting funcion (equation 6) to each FLAMINGO baryonic model with the best-fitting parameter value given in Table 1. For comparison, the coloured dotted lines indicate the $A_{\rm mod}(k)$ functions Amon & Efstathiou (2022) and Preston et al. (2023) inferred by combining observational data sets.

The total matter power spectra in the hydrodynamical and gravity-only simulations are measured as described by Schaller et al. (2025).[2]

3 ANALYTIC FORMULATION OF THE BARYONIC RESPONSE

3.1 The $A_{\rm mod}$ correction extracted from FLAMINGO

We start by computing the correction function $A_{\rm mod}(k)$ at $z = 0$ for the FLAMINGO simulations by inverting equation (1). To compute the linear matter power spectra for our cosmology, we use the CLASS (Lesgourgues 2011) package and add the Mead et al. (2021) halo model for the non-linear component. Note that we do not make use of the baryonic correction their model offers. We could alternatively have used the DMO simulations from the FLAMINGO suite to obtain the non-linear matter power spectrum. Using both the linear and non-linear power spectra from commonly used tools exemplifies how the correction we derive here can be applied in practice without the need for additional FLAMINGO data. A comparison between the FLAMINGO predictions and the Mead et al. (2021) model is nevertheless shown in Appendix A.

The $A_{\rm mod}(k)$ corrections extracted from the simulations are shown as dashed lines in Fig. 1. The different line colours correspond to the corrections extracted from the various FLAMINGO simulations calibrated to reproduce shifted versions of the gas fraction in clusters inferred from X-ray and weak-lensing data. For models where no simulation data exist, we made use of the FLAMINGO baryon response emulator introduced by Schaller et al. (2025). The FLAMINGO simulations are labelled by the number of standard deviations by which the observed cluster gas fractions that the simulations were calibrated to were shifted (see Kugel et al. 2023). Rather than considering the global shift of the data set, it may be useful to instead label the models by the gas fractions measured at a specific halo mass. Such a mapping is given in fig. 4 of Schaller et al. (2025).

For comparison, the constant $A_{\rm mod}$ obtained by Amon & Efstathiou (2022) and Preston et al. (2023), as well as the binned version from Preston et al. (2023), is shown as dotted lines in Fig. 1. Their estimates were constructed by combining CMB results with weak-lensing data and demanding a consistent cosmology fit. Note that at $k \lesssim 0.2\ h\,{\rm Mpc}^{-1}$, the value of $A_{\rm mod}(k)$ is not important for the discussion that follows as the difference between the linear and non-linear power spectra is small. This leads to large variations in $A_{\rm mod}(k)$ having only a minor impact on the total matter power spectrum. Comparing the FLAMINGO curves to the ones obtained by Amon and Efstathiou (2022) and Preston et al. (2023), we see that $A_{\rm mod}$ from the simulation is *larger*, meaning that the effect of baryons on the matter power spectrum is *smaller* than their analysis obtained. This matches the results of Schaller et al. (2025) and McCarthy et al. (2025). Note also that, beyond the differences in normalization, the shape of the binned $A_{\rm mod}$ by Preston et al. (2023) differs from what is predicted by the simulations.

3.2 Analytic fitting functions

A visual inspection of the dashed curves in Fig. 1 suggests that the $A_{\rm mod}(k)$ correction extracted from the various FLAMINGO simulations at $k \lesssim 10\ h\,{\rm Mpc}^{-1}$ can be approximated by a sigmoid curve. We choose to write:

$$A_{\rm mod}(k) = A_{\rm low} + \frac{1}{2}\,(1 - A_{\rm low})\left[1 - \tanh\left(\frac{\log_{10}(k/k_{\rm mid})}{\sigma_{\rm mid}}\right)\right] \quad (5)$$

and to fit the three free parameters to the curves extracted from the simulations. Specifically, we use a least-square approach and use the range $k = [0.03, 10]\ h\,{\rm Mpc}^{-1}$ to obtain the best-fitting parameters. Note that the choice of sigmoid guarantees that $A_{\rm mod}(k) = 1$ on large scales. As a result of this fitting exercise, we noticed that the values of the parameters $\sigma_{\rm mid}$ and $A_{\rm low}$ barely varied when fitting our function to the $A_{\rm mod}(k)$ data extracted from the runs shown in Fig. 1. We thus decided to keep the values of these two parameters fixed to the mean values of all the runs analysed ($\sigma_{\rm mid} = 0.656$ and $A_{\rm low} = 0.745$). Our parametrization of $A_{\rm mod}(k)$ thus reduces to a simple one-parameter family:

$$A_{\rm mod}(k) = 0.745 + 0.1275\left[1 - \tanh\left(\frac{\log_{10}(k/k_{\rm mid})}{0.656}\right)\right]. \quad (6)$$

The values of the best-fitting $k_{\rm mid}$ parameter for the individual FLAMINGO simulations in which the target gas fractions for the model calibration were varied are given in Table 1 and the resulting functions are shown using solid lines on Fig. 1. As can be seen, our single-parameter sigmoids are a good fit to the $A_{\rm mod}(k)$ extracted from the simulations up to the wavenumber $k \approx 10\ h\,{\rm Mpc}^{-1}$ where the simulation predictions turn over and show an increase. This is the scale where the contraction due to baryonic cooling of the haloes matters and is also beyond the range relevant to the current and next-generation data sets.

[2]The raw matter power spectra for all the simulations of the FLAMINGO suite have been made publicly available on the website of the project: https://flamingo.strw.leidenuniv.nl/.

Table 1. The values of the parameter for the best-fitting $A_{\rm mod}(k)$ correction function (equation 6) to simulations from the FLAMINGO suite that were calibrated to different shifted versions of the observed gas fractions. The first column gives the simulation names used by Schaye et al. (2023). The names post-fixed with a † superscript indicate simulations that do not exists and whose response was obtained using the Gaussian-process emulator introduced by Schaller et al. (2025).

Simulation name	$k_{\rm mid}$ ($h\,{\rm Mpc}^{-1}$)
fgas-8σ	1.813 ± 0.004
fgas$-6\sigma^\dagger$	2.167 ± 0.004
fgas-4σ	2.736 ± 0.005
fgas$-3\sigma^\dagger$	3.124 ± 0.006
fgas-2σ	3.614 ± 0.008
fgas$-1\sigma^\dagger$	4.262 ± 0.009
fgas$+0\sigma$ (L1_m9)	5.175 ± 0.012
fgas$+1\sigma^\dagger$	6.572 ± 0.016
fgas$+2\sigma$	8.968 ± 0.026

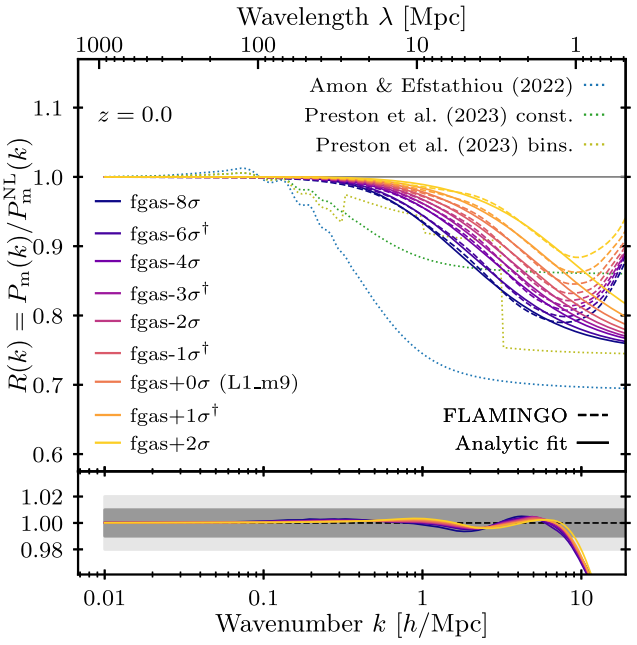

Figure 2. The baryonic response of the matter power spectrum (equation 3) as a function of wavenumber at $z = 0$ obtained using the $A_{\rm mod}$ correction (equation 1) and our analytic function (equation 6) with the parameters for each FLAMINGO model given in Table 1 (solid lines). The dashed lines in matching colours correspond to the data extracted from the individual simulations fitted to various gas fractions in groups and clusters (or from an emulator, indicated by a dagger). For comparison, the coloured dotted lines indicate the response functions that Amon & Efstathiou (2022) and Preston et al. (2023) inferred by combining observational datasets. The bottom panel shows the ratio between our analytic model and the direct simulation prediction. The shaded regions correspond to fractional errors of 1 per cent and 2 per cent, respectively. For the different models and for all $k < 10\,h\,{\rm Mpc}^{-1}$, the analytic formulation reproduces the FLAMINGO results to close to (or better than) 1 per cent relative accuracy.

3.3 The baryonic response

Having constructed a simple analytic expression for $A_{\rm mod}(k)$, we turn our attention to the baryonic response (equation 3) it generates. In Fig. 2, we show using solid lines the response as a function of wavenumber at $z = 0$. The different colours correspond to the various FLAMINGO models, as indicated in the legend. The dashed lines in the background show the direct results of the corresponding simulations or the results of the Schaller et al. (2025) emulator where no simulation was run. For scales $k \lesssim 10\,h\,{\rm Mpc}^{-1}$, our approximation is an excellent match to the simulation (or emulator) results with all models matching the simulations they are fitted to to better (or close to) 1 per cent accuracy. This is of course not unexpected since we explicitly constructed the $A_{\rm mod}(k)$ sigmoid to achieve this; however, the exact quantitative agreement at the level of precision we reached with a simple one-parameter function was not necessarily to be expected a priori. As a point of comparison, the responses inferred by Amon and Efstathiou (2022) and Preston et al. (2023) are shown using dotted lines. Additional comparisons between the FLAMINGO results and the ones inferred from other simulations or by analysis of observational data sets can be found in the study by Schaller et al. (2025; their figs. 11 and 13, respectively).

The fact that the response inferred from FLAMINGO deviates from the one obtained by Amon & Efstathiou (2022) implies that the simulations do not fit the data they used and do not resolve the S8 tension (see also McCarthy et al. 2023, 2025; Elbers et al. 2025). This is, at least in part, due to Amon & Efstathiou (2022) forcing the baryonic effects to solve the tension between KiDS lensing and the CMB and hence demanding a rather dramatic correction to the matter power spectrum while the FLAMINGO calibration strategy was to match the observed gas fraction in clusters. Note however that the original tension between KiDS lensing and the CMB seems to have dissolved in more recent analysis of the weak-lensing data (Wright et al. 2025).

3.4 Evolution with redshift

The first key assumption underlying the approach of writing the total matter power spectrum in the form of equation (1) is that the function $A_{\rm mod}$ is independent of redshift. Having fitted $A_{\rm mod}(k)$ to our $z = 0$ simulation results, we now apply that fit at higher redshift. In this process, we keep $A_{\rm mod}$ as fitted in Section 3.2 but compute $P_{\rm m}^{\rm L}(k, z)$, $P_{\rm m}^{\rm NL}(k, z)$, and thus $\beta^{\rm NL}(k, z)$, from CLASS and the Mead et al. (2021) model at the redshift of interest. We then compute the baryonic response using equation (3) for our various FLAMINGO models and show the results at three different redshifts in Fig. 3, where we compare it to the raw data extracted from the simulations. From left to right, we show results at $z = 0.5$, 1, and $z = 2$. The solid lines correspond to our analytic model while the dashed lines show the results of the simulations (or the emulator).

As can be seen by comparing the solid lines in the different panels, the analytic correction displays only a small amount of evolution with redshift. The simulation results show a more significant evolution, especially at $z > 1$. At $z \leq 1$, the analytic $A_{\rm mod}$ model matches the simulation results at the 2 per cent level up to scales $k = 3\ h \cdot {\rm Mpc}^{-1}$ for all the models shown here. We recall that the functional fit was only performed at $z = 0$. It is thus quite remarkable that the simple one-parameter sigmoid is sufficient to capture the behaviour of simulations with different levels of baryonic response over a wide range of redshifts.

We also performed the same analysis for all the intermediate redshifts where we have data ($\Delta z = 0.05$) and measured the maximal relative error ϵ between the analytic fit and the simulation (or emulator). Over the range $k \leq 1\,h\,{\rm Mpc}^{-1}$, we get

$$\epsilon < 1 \text{ per cent for } z \leq 1 \quad \text{and} \quad \epsilon < 2 \text{ per cent for } z \leq 1.5.$$

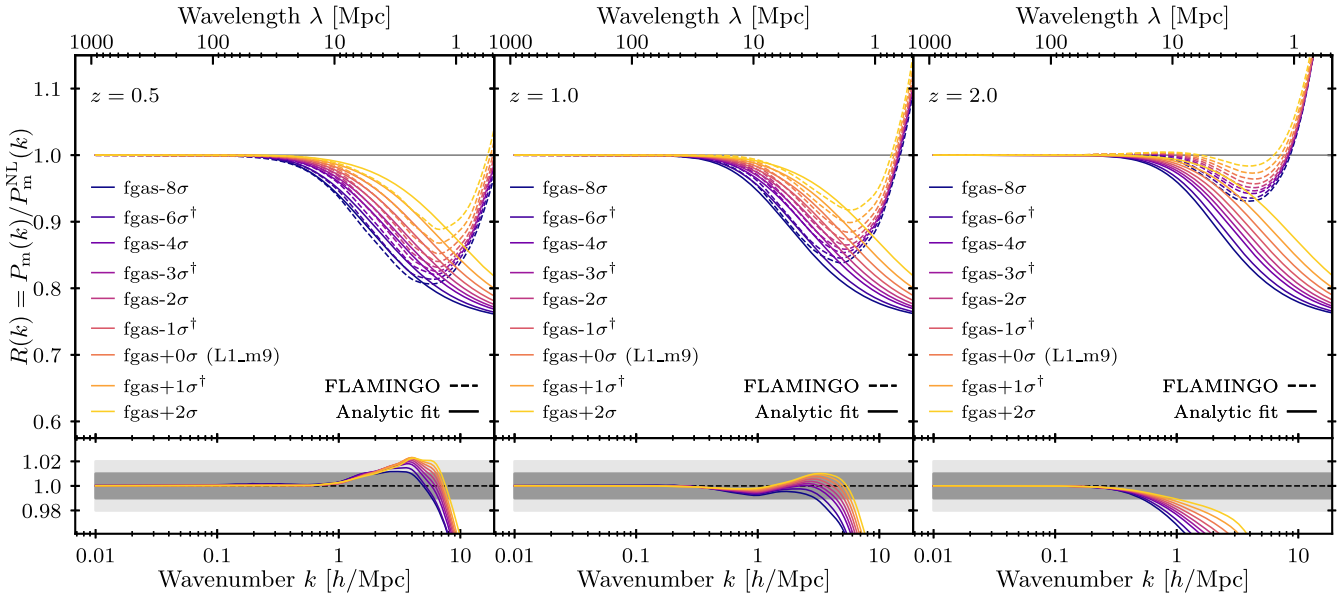

Figure 3. Same as Fig. 2 but at $z = 0.5$, 1, and 2 (from left to right). Despite the fit having been performed at $z = 0$, our analytic fit is in excellent agreement with the response extracted from the simulations at $z \leq 1$. This confirms the assumption that, at the level of precision required here and for this range of redshifts, $A_{\rm mod}(k, z)$ does not require a redshift dependence.

Table 2. The values of the cosmological parameters for the different simulations of the FLAMINGO suite used in this study. All simulations assume a flat Lambda cold dark matter (ΛCDM) Universe including massive neutrinos with $N_{\rm eff} = 3.044$ effective relativistic neutrino species at high redshift and with an amount of radiation corresponding to $T_{\rm CMB} = 2.7255$ K. For the simulations with decaying CDM (DCDM), the $\Omega_{\rm cdm}$ corresponds to the sum of the present-day densities of DCDM and dark radiation. For these models, the last column shows the dark matter decay rate, Γ, in units of 100 km s^{-1} Mpc^{-1} $= H_0/h$.

Simulation name	h	$\Omega_{\rm m}$	$\Omega_{\rm cdm}$	$\Omega_{\rm b}$	$\sum m_\nu$	σ_8	$10^9 A_{\rm s}$	$n_{\rm s}$	$\Gamma h/H_0$
D3A (L1_m9)	0.681	0.306	0.256	0.0486	0.06 eV	0.807	2.099	0.967	–
Planck	0.673	0.316	0.265	0.0494	0.06 eV	0.812	2.101	0.966	–
LS8	0.682	0.305	0.256	0.0473	0.06 eV	0.760	1.836	0.965	–
PlanckNu0p24Fix	0.673	0.316	0.261	0.0494	0.24 eV	0.769	2.101	0.966	–
PlanckNu0p24Var	0.662	0.328	0.271	0.0510	0.24 eV	0.772	2.109	0.968	–
PlanckDCDM12	0.673	0.274	0.246	0.0494	0.06 eV	0.794	2.101	0.966	0.12
PlanckDCDM24	0.673	0.239	0.229	0.0494	0.06 eV	0.777	2.101	0.966	0.24

Extending the range to $k \leq 3\,h\,{\rm Mpc}^{-1}$, we find

$\epsilon < 2$ per cent for $z \leq 1$ and $\epsilon < 5$ per cent for $z \leq 1.5$.

These maximal errors are measured across all the simulation variations shown in Figs 1–3 with the value of the single free parameter value of the fitting function given in Table 1.

We thus conclude that our one-parameter analytic fit to $z = 0$ data is sufficiently accurate over a wide range of redshift and scales for a large range of applications.

3.5 Background cosmology dependence

The second key assumption underlying the approach of writing the total matter power spectrum in the form of equation (1) is that the function $A_{\rm mod}$ is independent of the chosen background cosmology. The dependence of the total matter power spectrum on the cosmological parameters is then entirely captured by the effects the parameters have on $P_{\rm m}^{\rm L}$ and $P_{\rm m}^{\rm NL}$ (i.e. can be obtained from DMO simulations).

The fitting function we obtained above was constructed using FLAMINGO simulations that all adopt our fiducial cosmology (D3A). We now compare the fit to the other models that are part of the FLAMINGO suite. To this end, we keep $A_{\rm mod}$ as fitted in Section 3.2 but compute $P_{\rm m}^{\rm L}(k, z)$, $P_{\rm m}^{\rm NL}(k, z)$, and thus $\beta^{\rm NL}(k, z)$, from CLASS and the Mead et al. (2021) model for the different cosmologies in the FLAMINGO suite whose parameter values are given in Table 2. We then obtain the baryonic response of the matter power spectrum and show the results at $z = 0$ using solid lines in the left panel of Fig. 4. We compare our analytic model to the direct results of the simulations using dashed lines with the same colours.

Putting aside the two models featuring decaying dark matter (PlanckDCDM12 and PlanckDCDM24), we see that the analytic expression matches the results of the simulations extremely well. As we performed the fit only for our fiducial cosmology, this was not guaranteed a priori. We see also that there is very little dependence of the baryonic response on the cosmology. This was already noted by Schaller et al. (2025; their fig. 10) and can be explained by the model proposed by Elbers et al. (2025) who linked the changes in the response to changes in the halo mass–concentration relation. However, we caution that the range of cosmologies explored here does not include models that lead to large variations in this relation and thus in the response. Two important type of parameter variations have nevertheless been explored: those leading to scale-dependent (changes in $n_{\rm s}$, $\sum m_\nu$) and

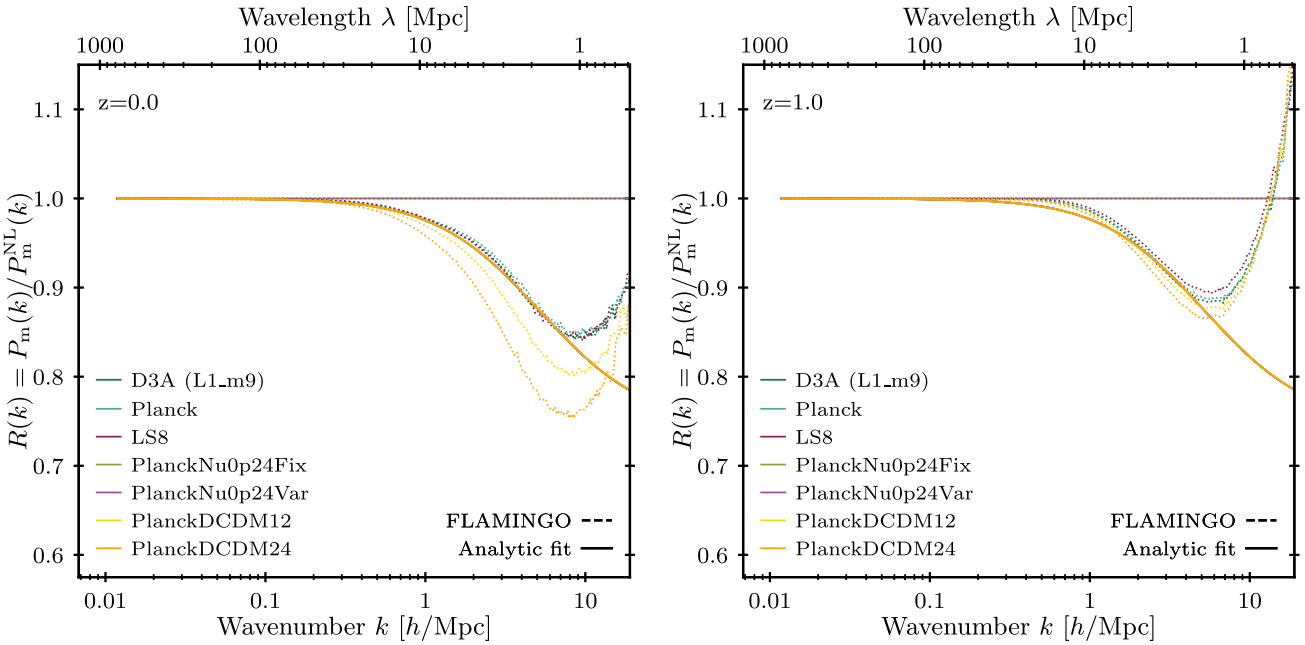

Figure 4. Same as Fig. 2 but for different background cosmologies in the FLAMINGO suite, as indicated in the legend both at $z = 0$ (left) and $z = 1$ (right). For the five cosmologies that do not involve decaying dark matter, the analytic formulation yields excellent results (the solid and dashed lines overlap), especially at $z = 0$. This confirms the assumption that the function $A_{\rm mod}(k)$ does not require a dependence on the choice of background cosmology to match our simulations. We caution, however, that the FLAMINGO suite only covers a small range of cosmology variations. See the text for the discussion of the two models including decaying dark matter.

scale-independent (changes in $\Omega_{\rm m}, \sigma_8$) effects on the linear power spectrum.

We also note that we do not explore models that feature significant changes in the ratio $\Omega_{\rm b}/\Omega_{\rm m}$. We leave such explorations to future studies that make use of a wider range of cosmological models.

It is interesting to note that, assuming a fixed $A_{\rm mod}$, the lack of a cosmology dependence of the baryon response implies (through equation (4) that the non-linear response $\beta^{\rm NL}$ itself is also insensitive to the choice of cosmology. This is further expanded upon in Appendix A.

On the scale of interest, $\beta^{\rm NL}$ is dominated by the one-halo term, which displays little cosmology-dependence in halo models. It is thus interesting to repeat the comparison at higher redshift where this term is smaller. We show the response obtained in the simulations and using our analytic model at $z = 1$ in the right panel of Fig. 4. For the simulations (dashed lines), a greater level of cosmology-dependence than at $z = 0$ can be seen. This is, however, not captured by the analytic model (solid lines). The halo model does not capture the cosmology-dependence of the one-halo to two-halo transition. More advanced modelling of $\beta^{\rm NL}$ in the future might reconcile the simulations and the model. We note, however, that the differences seen here are nonetheless only at the 2 per cent level for $k < 3\,h\,{\rm Mpc}^{-1}$.

Turning now our attention to the two models with decaying dark matter, we see that the analytic fit to $A_{\rm mod}$ predicts the same level of response as in the other cosmological models. This is in tension with the simulation results (dashed lines), which predict a rather different response at $z = 0$. This is in part due to the non-linear model used to compute $P_{\rm m}^{\rm NL}$ not reproducing the simulations in this regime (see Appendix A) and in part due to the assumption, made when constructing $A_{\rm mod}$, that the correction does not depend on cosmology breaking down. This can be verified by using the results of the DMO model as input $P_{\rm m}^{\rm NL}$. When doing this, the analytic approximation also differs from the hydrodynamical simulation results (not shown). At $z = 1$ (right panel), the responses extracted from the simulations with decaying dark matter display a behaviour closer to the other cosmologies, and is hence captured better by our analytic model than at $z = 0$.

3.6 Other AGN feedback implementation

We have so far considered the fiducial implementation of AGN feedback in the FLAMINGO suite. The set of FLAMINGO simulations also includes models where the mode of injection of energy from the AGN activity was altered from thermally driven winds to collimated injection following the jet model of Huško et al. (2022). Despite these models being calibrated to the same set of observables as the simulations using the thermal isotropic energy injection scheme, these models display differences in the response the feedback imparts onto the matter power spectrum (Schaye et al. 2023; Schaller et al. 2025). It is thus interesting to extend our analysis to these models in order to provide $A_{\rm mod}(k)$ functions covering additional plausible scenarios.

We employ the same strategy as for the simulations using the fiducial AGN feedback implementation (Section 3.2) and fit equation (5) to the $A_{\rm mod}(k)$ data extracted from the various simulations with jet AGN feedback (or from the emulator when simulations do not exist). However, unlike in the earlier case, we find that the three free parameters have to be varied jointly to fit the simulations. The best-fitting parameters are provided in Table 3.

From the best-fitting $A_{\rm mod}(k)$ curves, we construct the baryonic response of the matter power-spectrum and show the results in Fig. 5. The dashed lines show the response extracted directly from the simulations or emulator with the different line colours indicating the number of sigma by which the gas fractions were shifted before

Table 3. The values of the parameters for the best-fitting $A_{\rm mod}(k)$ correction function (equation 5) to simulations from the FLAMINGO suite that were calibrated to different shifted versions of the observed gas fractions but using the collimated jet AGN feedback implementation. The first column gives the simulation names used by Schaye et al. (2023). The names post-fixed with a superscript † indicate simulations that do not exist and whose response was obtained using the Gaussian-process emulator introduced by Schaller et al. (2025).

Simulation name	$k_{\rm mid}$ ($h\,{\rm Mpc}^{-1}$)	$\sigma_{\rm mid}$ (−)	$A_{\rm low}$ (−)
Jet_fgas−8$\sigma^\dagger$	1.530 ± 0.012	0.964 ± 0.003	0.668 ± 0.001
Jet_fgas−6$\sigma^\dagger$	1.934 ± 0.020	0.979 ± 0.004	0.688 ± 0.001
Jet_fgas−4σ	2.995 ± 0.046	1.006 ± 0.005	0.700 ± 0.001
Jet_fgas−3$\sigma^\dagger$	3.936 ± 0.077	1.010 ± 0.006	0.706 ± 0.001
Jet_fgas−2$\sigma^\dagger$	5.195 ± 0.131	0.994 ± 0.006	0.714 ± 0.002
Jet_fgas−1$\sigma^\dagger$	6.489 ± 0.205	0.942 ± 0.007	0.734 ± 0.002
Jet_fgas+0σ	6.739 ± 0.230	0.817 ± 0.008	0.782 ± 0.002
Jet_fgas+1$\sigma^\dagger$	4.937 ± 0.105	0.534 ± 0.007	0.870 ± 0.001
Jet_fgas+2$\sigma^\dagger$	4.569 ± 0.034	0.204 ± 0.005	0.937 ± 0.000

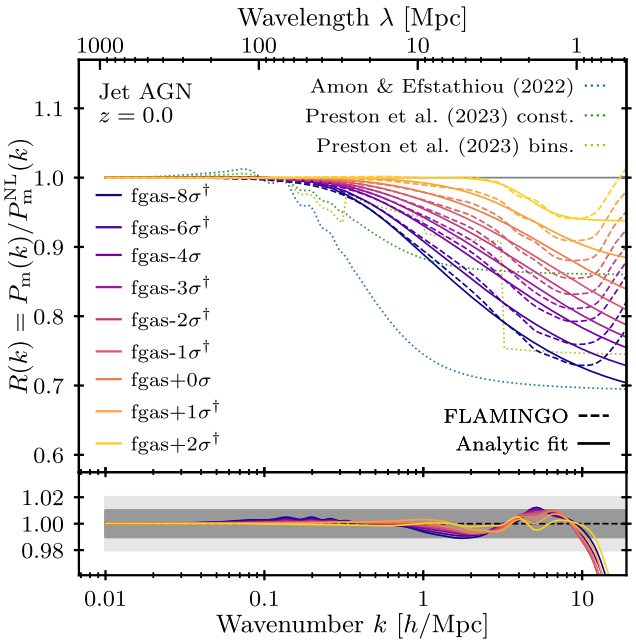

Figure 5. Same as Fig. 2 but for models which used the collimated jet implementation for AGN feedback instead of the isotropic mode (solid lines). The dashed lines in matching colours correspond to the data extracted from the individual simulations fitted to various gas fractions in groups and clusters (or from an emulator, indicated by a dagger). To obtain a good fit to the simulation results, we used the more general three-parameters version of $A_{\rm mod}$ (equation 5) with the values of the best-fitting parameters given in Table 3. The slightly more complex shape of the response function in the case of the collimated jet model in FLAMINGO can also be captured by our sigmoid function, albeit at the cost of extra free parameters.

the calibration of the simulations. The solid lines in matching colours show the best-fitting $A_{\rm mod}(k)$ function (equation 5) using the best-fitting parameters of Table 3. As can be seen, the model is generally a good fit with a relative error (bottom panel) of $\lesssim 1$ per cent (dark grey region) up to $k \approx 10\,h\,{\rm Mpc}^{-1}$.

We conclude this exercise by noting that our simple functional form is sufficient to capture a range of baryon response behaviour, albeit at the cost of extra free parameters.

4 CONCLUSIONS

In this study, we used the hydrodynamical simulations from the FLAMINGO project (Kugel et al. 2023; Schaye et al. 2023) to extract fitting functions for the $A_{\rm mod}(k, z)$ modifier that Amon & Efstathiou (2022) introduced as a simple and fast means to model the effect of baryons on the total matter power spectrum. Here $A_{\rm mod}$ is the ratio between (a) the difference between the non-linear gravity-only and linear matter power spectra and (b) the difference between the true total non-linear matter power spectrum and the linear matter power spectrum (equation 1). Amon & Efstathiou (2022) assumed $A_{\rm mod}(k)$ is constant, which Preston et al. (2023) relaxed to assuming that it is independent of redshift and cosmology

By inspecting the $A_{\rm mod}(k)$ extracted from the various simulations in the FLAMINGO suite, we demonstrated that a constant is a poor approximation (Fig. 1). We found that a sigmoid function with a single free parameter (equation 6) is able to reproduce the $A_{\rm mod}(k)$ data extracted from the $z = 0$ simulations calibrated to match shifted versions of the observed gas content in clusters (Fig. 1). We then showed that this approximation leads to a baryonic response of the matter power spectrum matching the raw output of the FLAMINGO simulations to better than 1 per cent up to wavenumbers $k \leq 10\,h\,{\rm Mpc}^{-1}$ (Fig. 2).

We then tested the key assumptions underlying the $A_{\rm mod}$ approach. We found that the $A_{\rm mod}$ function does *not* need to depend on redshift for $z \leq 1$ (Fig. 3). At $k \leq 3\,h\,{\rm Mpc}^{-1}$, the maximal relative error with respect to the FLAMINGO results is smaller than 2 per cent at redshifts $z \leq 1$.

We also found that, within the range of cosmologies available in the FLAMINGO suite, the $A_{\rm mod}$ function does *not* need to depend on the choice of cosmology (Fig. 4). The situation is more complex for models with decaying dark matter and, possibly, for models where the difference with our base ΛCDM cosmology increases. In particular, we note that we have not explored models where the ratio $\Omega_{\rm b}/\Omega_{\rm m}$ varies significantly.

Finally, we explored a wider range of AGN feedback implementations and found that our sigmoid function can also accommodate models in the FLAMINGO suite that use AGN jet feedback instead of the fiducial thermally driven AGN feedback (Fig. 5) albeit at the cost of extra parameters in the sigmoid function.

Having verified the two key assumptions that $A_{\rm mod}(k)$ does not evolve and does not depend on cosmology, at least for $z < 1$, CDM, and limited variations in cosmology, we confirm that the approach proposed by Amon & Efstathiou (2022) is valid and able to reproduce the results of complex cosmological simulations, provided a sigmoid function is used for $A_{\rm mod}(k)$. Our analytic function thus provides a very efficient way, based on a single parameter linked to the gas fraction in clusters, to obtain an excellent estimate of the effect of baryons on the matter power spectrum at redshifts and scales relevant to the analyses of current surveys.

ACKNOWLEDGEMENTS

We thank the anonymous referee for their helpful comments. This work used the DiRAC@Durham facility managed by the Institute for Computational Cosmology on behalf of the STFC DiRAC HPC Facility (www.dirac.ac.uk). The equipment was funded by BEIS capital funding via STFC capital grants ST/K00042X/1, ST/P002293/1, ST/R002371/1, and ST/S002502/1, Durham University, and STFC operations grant ST/R000832/1. DiRAC is part of the National e-Infrastructure.

DATA AVAILABILITY

The raw matter power spectra used in this paper are available on the FLAMINGO project's web page.[3]

REFERENCES

Abbott T. M. C. et al., 2022, Phys. Rev. D, 105, 023520
Amon A., Efstathiou G., 2022, MNRAS, 516, 5355
Angulo R. E., Zennaro M., Contreras S., Aricò G., Pellejero-Ibañez M., Stücker J., 2021, MNRAS, 507, 5869
Aricò G., Angulo R. E., Contreras S., Ondaro-Mallea L., Pellejero-Ibañez M., Zennaro M., 2021, MNRAS, 506, 4070
Asgari M., Mead A. J., Heymans C., 2023, Open J. Astrophys., 6, 39
Bahé Y. M. et al., 2022, MNRAS, 516, 167
Bigwood L., Bourne M. A., Irsic V., Amon A., Sijacki D., 2025, preprint (arXiv:2501.16983)
Bocquet S., Heitmann K., Habib S., Lawrence E., Uram T., Frontiere N., Pope A., Finkel H., 2020, ApJ, 901, 5
Booth C. M., Schaye J., 2009, MNRAS, 398, 53
Borrow J., Schaller M., Bower R. G., Schaye J., 2022, MNRAS, 511, 2367
Braspenning J. et al., 2024, MNRAS, 533, 2656
Braspenning J., Schaye J., Schaller M., Kugel R., Kay S. T., 2025, MNRAS, 536, 3784
Chaikin E., Schaye J., Schaller M., Benítez-Llambay A., Nobels F. S. J., Ploeckinger S., 2023, MNRAS, 523, 3709
Chen Z., Yu Y., Han J., Jing Y. P., 2025, preprint (arXiv:2502.11160)
DeRose J. et al., 2019, ApJ, 875, 69
Debackere S. N. B., Schaye J., Hoekstra H., 2020, MNRAS, 492, 2285
Delgado A. M. et al., 2023, MNRAS, 526, 5306
Elbers W., Frenk C. S., Jenkins A., Li B., Pascoli S., 2021, MNRAS, 507, 2614
Elbers W., Frenk C. S., Jenkins A., Li B., Pascoli S., 2022, MNRAS, 516, 3821
Elbers W. et al., 2025, MNRAS, 537, 2160
Euclid Collaboration et al., 2019, MNRAS, 484, 5509
Ferreira T., Alonso D., Garcia-Garcia C., Chisari N. E., 2024, Phys. Rev. Lett., 133, 051001
Giri S. K., Schneider A., 2021, J. Cosmol. Astropart. Phys., 2021, 046
Hahn O., Rampf C., Uhlemann C., 2021, MNRAS, 503, 426
Heitmann K. et al., 2016, ApJ, 820, 108
Huško F., Lacey C. G., Schaye J., Schaller M., Nobels F. S. J., 2022, MNRAS, 516, 3750
Kugel R. et al., 2023, MNRAS, 526, 6103
Kumar A. et al., 2025, preprint (arXiv:2501.19327)
Lawrence E. et al., 2017, ApJ, 847, 50
Le Brun A. M. C., McCarthy I. G., Schaye J., Ponman T. J., 2014, MNRAS, 441, 1270
Lesgourgues J., 2011, preprint (arXiv:1104.2932)
Lewis A., Challinor A., Lasenby A., 2000, ApJ, 538, 473
McCarthy I. G., Schaye J., Bird S., Le Brun A. M. C., 2017, MNRAS, 465, 2936
McCarthy I. G. et al., 2023, MNRAS, 526, 5494
McCarthy I. G. et al., 2025, MNRAS, 540, 143
Mead A. J., Peacock J. A., Heymans C., Joudaki S., Heavens A. F., 2015, MNRAS, 454, 1958
Mead A. J., Heymans C., Lombriser L., Peacock J. A., Steele O. I., Winther H. A., 2016, MNRAS, 459, 1468
Mead A. J., Tröster T., Heymans C., Van Waerbeke L., McCarthy I. G., 2020, A&A, 641, A130
Mead A. J., Brieden S., Tröster T., Heymans C., 2021, MNRAS, 502, 1401
Pakmor R. et al., 2023, MNRAS, 524, 2539
Ploeckinger S., Schaye J., 2020, MNRAS, 497, 4857
Preston C., Amon A., Efstathiou G., 2023, MNRAS, 525, 5554
Schaller M. et al., 2024, MNRAS, 530, 2378
Schaller M., Schaye J., Kugel R., Broxterman J. C., van Daalen M. P., 2025, MNRAS, 539, 1337
Schaye J., Dalla Vecchia C., 2008, MNRAS, 383, 1210
Schaye J. et al., 2023, MNRAS, 526, 4978
Schneider A., Teyssier R., 2015, J. Cosmol. Astropart. Phys., 2015, 049
Seljak U., 2000, MNRAS, 318, 203
Semboloni E., Hoekstra H., Schaye J., 2013, MNRAS, 434, 148
Smith R. E. et al., 2003, MNRAS, 341, 1311
Springel V., Di Matteo T., Hernquist L., 2005, ApJ, 620, L79
Storey-Fisher K., Tinker J. L., Zhai Z., DeRose J., Wechsler R. H., Banerjee A., 2024, ApJ, 961, 208
Takahashi R., Sato M., Nishimichi T., Taruya A., Oguri M., 2012, ApJ, 761, 152
Wiersma R. P. C., Schaye J., Theuns T., Dalla Vecchia C., Tornatore L., 2009, MNRAS, 399, 574
Wright A. H. et al., 2025, preprint (arXiv:2503.19441)

APPENDIX A: COMPARISON OF NON-LINEAR RESPONSE FOR DIFFERENT COSMOLOGIES

In this appendix, we compare the non-linear boost, $\beta^{\rm NL}(k, z)$ (equation 2) extracted from DMO FLAMINGO simulations assuming different cosmologies to the ones obtained using the (Mead et al. 2021) halo model as implemented in the CLASS code (Lesgourgues 2011). In both cases, we use the CLASS code to obtain the linear power spectra. The boosts as a function of wavelength extracted from the DMO FLAMINGO runs with different cosmologies are shown in the top panel of Fig. A1 using solid lines. The dashed lines in matching colours indicate the non-linear boosts obtained from the halo models. The middle panel shows the ratio of the FLAMINGO boost to the (Mead et al. 2021) one.

Putting the two models with decaying dark matter aside, we find that the halo model and simulations agree to within a few per cent over the whole range of scales relevant to current cosmology surveys ($k < 10\ h \cdot \mathrm{Mpc}^{-1}$). The two models with decaying dark matter display a much stronger non-linear boost in the halo model than in the FLAMINGO simulations. This is not unexpected, as such cosmologies were not part of the set used to design and test the Mead et al.'s (2021) halo model.

The bottom panel of Fig. A1 shows the ratio of the non-linear boost in our different cosmologies to the one extracted from the fiducial cosmology (D3A). All the boosts here are extracted from the simulations. As expected from the analysis in Section 3.5, we find that the non-linear boost only has a mild dependence on cosmology.

[3] https://flamingo.strw.leidenuniv.nl/

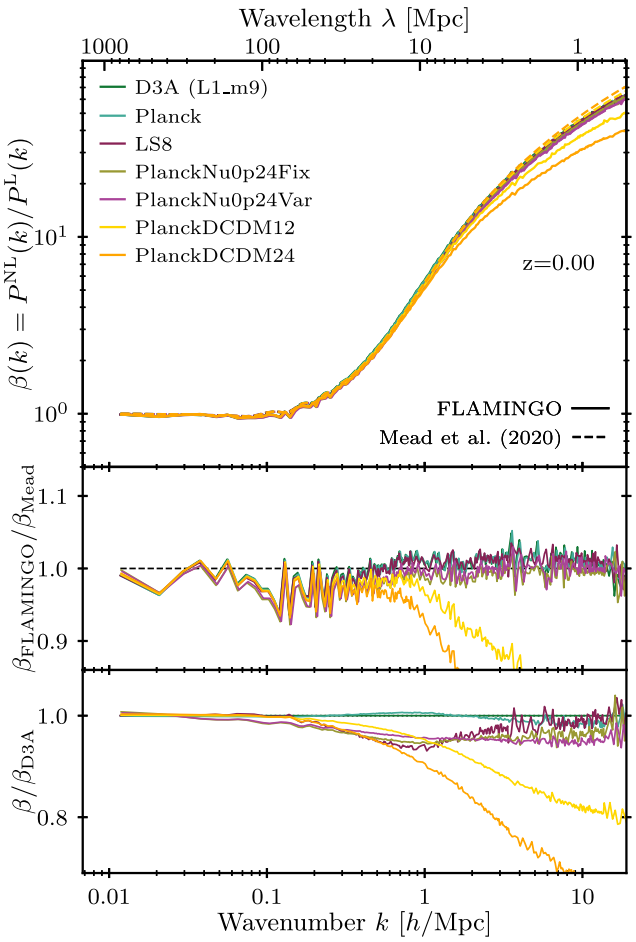

Figure A1. *Top*: The ratio of the non-linear and linear matter power spectra (equation 2) for seven different cosmologies (different colours) in the FLAMINGO suite as a function of wavenumber. The solid lines correspond to the results of the DMO simulations and the dashed lines in matching colours show the results of the Mead et al.'s (2021) halo model. For both sets of lines, the linear matter power spectrum was computed using the CLASS code (Lesgourgues 2011). *Middle*: The ratio of the non-linear response predicted by FLAMINGO and the halo model. Apart from the decaying dark matter models, over the entire range of scales relevant to our study, the simulations agree with the halo model to within a few per cent. *Bottom*: The ratio of the non-linear response in the various cosmological models to the response in our fiducial cosmology (D3A) for the DMO FLAMINGO runs. The decaying dark matter models display a significantly different non-linear response from the other cosmological models.

This paper has been typeset from a TEX/LATEX file prepared by the author.